Upregulation of pro-angiogenic genes in tumor cells that promote an invasive and proliferative phenotype are found in poor responders to bevacizumab therapy.

Roshan Lodha[a,b], Candece Gladson[b,*]
[a]Lerner College of Medicine, Cleveland Clinic, 9501 Euclid Avenue, Cleveland, Ohio 44195
[b]Lerner Research Institute, Cleveland Clinic, 9500 Euclid Avenue, Cleveland, Ohio 44195

Abstract. Glioblastoma is the most common primary brain tumor in adults with a 15-month median overall-survival. After surgical resection and radio-chemotherapy, tumor recurrence occurs in more than 90% of patients. Therapies at recurrence include bevacizumab, a monoclonal antibody to vascular endothelial growth factor (VEGF) that blocks VEGF from binding to its receptor (VEGFR). While most patients do not show improvement in median overall survival, a small percent are good responders to bevacizumab with a longer overall-survival. Given the poor prognosis of glioblastoma, it is important to transition patients away from ineffective therapy as soon as possible. To find genetic contributors to ineffective bevacizumab response, we used computational methods to analyze existing RNA-sequencing data of human glioblastoma xenograft tumors propagated in athymic nude mice that were either poor or good responders to bevacizumab. We identified the angiogenic gene *CHRNA7* encoding the cholinergic receptor nicotinic alpha 7 subunit to be positively enriched in poor responders' tumor cells. In endothelial cells, the gene product of *CHRNA7*, α7-nAChR, regulates angiogenesis, whereas in non-brain cancer cells it has been reported to promote proliferation or migration. α7-nAChR expression, along with several other differentially expressed angiogenic factors, is regulated by the early growth response 1 (*EGR1*) transcription factor which is also upregulated in poor responders to bevacizumab, suggesting a more global epigenetic response to bevacizumab. In aggregate, our data suggest that poor responders to bevacizumab therapy show aberrant expression of endothelial genes that modulate pro-tumorigenic functions. These genes can be used as markers or for future downstream therapeutic target.

Keywords: bevacizumab, VEGF, *CHRNA7*, *EGR1*, glioblastoma, angiogenesis

***Candece Gladson, E-mail: gladsoc@ccf.org

1 Introduction

Grade IV glioma, or glioblastoma, is the most common primary brain tumor in adults with a median overall survival of just 14-15 months[1]. Despite primary treatment consisting of surgical resection followed by radiotherapy and chemotherapy, glioblastoma tumors relapse in over 90% of patients[2] and within 10 weeks on average[3]. There is currently no consensus for second-line therapy at recurrence; available options include new combinations of existing agents, clinical trials of new agents, and additional chemotherapy such as bevacizumab.

Glioblastoma is known to be a highly vascular, proliferative and invasive tumor[3]. One second-line option for therapy is to selectively target angiogenesis, with the goal of reducing nutrient supply to tumor cells to induce downstream necrosis. Due in part to the highly vascular nature of glioblastoma, the U.S. Food and Drug Administration (FDA) has approved single-agent use of bevacizumab as a second-line treatment for recurrent glioblastoma[4]. Bevacizumab is a humanized monoclonal antibody directed towards vascular endothelial growth factor-A (VEGF) and is a frequently used therapy for patients with recurrent glioblastoma. VEGF binds the VEGF receptors (VEGFR1 and 2) and signals for survival, proliferation and migration. Bevacizumab binds to circulating VEGF, as well as VEGF in the perivascular tumor niche[5], competitively preventing VEGF binding/signaling through its receptor (VEGFR) and thereby dampening angiogenesis and in some instances tumor progression[6]. Unfortunately, bevacizumab therapy alone improves overall patient survival in only a small percentage of patients[6]. Nevertheless, bevacizumab therapy is frequently used as a second line therapy as it mitigates brain edema and enhances the quality of life for patients. The mechanisms for resistance to anti-VEGF therapy in glioblastoma are still being identified. Therefore, identifying molecular drivers of poor response to bevacizumab therapy could aid in identifying patients with glioblastoma who would be poor responders, in order to transition such patients to alternative therapies. Here we use bulk RNA-sequencing techniques in tandem with immunohistochemical validation to highlight key genomic differences in differential responders to bevacizumab to propose potential novel therapeutic targets to be used in conjunction with bevacizumab therapy.

2 Methods

Human patient-derived xenograft tumors (PDXs) were propagated orthotopically in athymic nude mice. Good and poor responders to bevacizumab therapy were defined by their median overall survival time under bevacizumab treatment, with poor responders having a significantly shorter median overall survival time and good responders having no significant change or a significantly longer median overall survival time relative to the median. Tumor tissues were harvested at euthanasia for RNA-sequencing and immunohistochemical analysis.

2.1 Biochemical Methods

{TODO: define entire mouse experiment starting with point of origin for tumor samples}
{TODO: define IHC protocol}

2.2 Computational Analysis

RNA sequencing was done through the Illumina Next-Generation Sequencing (NGS) protocol {TODO: define exact NGS subprotocol with citation}. Following quality control, reads were processed through sequential pairing, alignment, and mapping. Subsequently processed reads were analyzed in R. Group factoring by PDX is shown in Supplemental Table 1.

All analysis was done using GalaxyProject (version 2.11.0) and R (version 4.0.3). Plots were generated using ggplot2 (version 3.3.5) and tables were generated using sjPlot (version 2.8.9).

2.2.1 Data loading, FASTQ extraction, and preprocessing

Data was retrieved in the SRA format from the NCBI directly onto GalaxyProject servers. Using the "Download and Extract Reads in FASTA/Q" workflow, fastq files were generated from the SRA. Reads were aligned to the hg19 reference genome using HISAT2. Specified parameters were unstranded paired-end data from a single interleaved dataset. Sample-level quality control was done through principal component analysis (PCA). Properly clustered points were retained for downstream analysis (Supplemental Figure 1A). A dendrogram was generated using euclidean distances between PCA points to better visualize outliers (Supplemental Figure 1B). Following PCA filtering, transcript-level filtering was done through mean-variance analysis (Supplemental Figure 2). Through hyperparameter optimization, a minimum read count of 350 reads was chosen as the cutoff threshold.

2.2.2 Biological analysis

Gene annotation was carried out in R using the ensembldb (version 2.12.1) package. EntrezID was paired to gene symbol. Differential gene expression analysis (DGE) was carried out using DESeq2 (version 3.13) started with loading samples using DESeqDataSetFromMatrix function.

Samples were normalized using the estimateSizeFactors function. Log fold change was shrunk using the ashr (version 1.10.0) lfcShrink function for better visualization.

Differentially expressed genes were sorted in descending order by $\frac{log_2 FC}{|log_2 FC|} \times adj(p)$, where $adj(p)$ represented the Benjamini-Hochberg adjusted p-value and FC represents the fold-change output in RNA levels from differential gene expression analysis. Subsequently, the GSEA function of clusterProfiler (version 3.16.1) was used to perform enrichment analysis of several curated gene sets, including KEGG, GO, and Hallmark. The gene sets were retrieved from msigdbr (version 7.4.1).

3 Results

3.1 Poor responders to anti-VEGF therapy delineate a distinct subtype of glioblastoma.

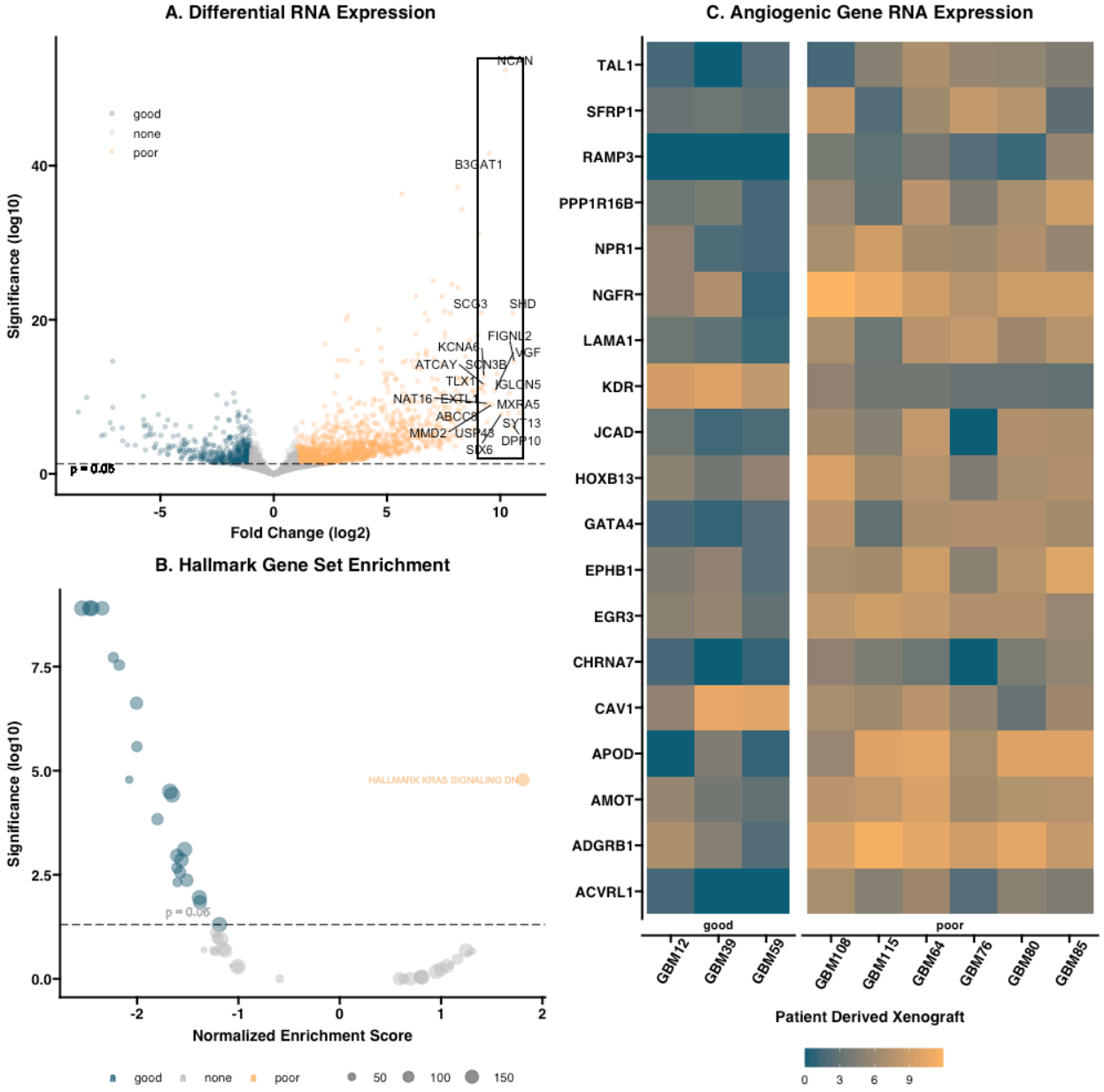

Figure 1 Across all plots, points in orange are enriched in poor responders to bevacizumab therapy while points in blue are enriched in good responders. A. Volcano plot of differential gene expression. Log2 fold change is plotted against negative log-scaled significance. Labeled points indicate the top 20 differentially expressed genes. B. Hallmark gene set enrichment analysis of responders to bevacizumab. Normalized enrichment score is plotted against negative log-scaled significance. The KRAS signaling downregulation gene set is labeled. C. Heatmap of log-scaled raw RNA-expression of differentially expressed angiogenic genes. Points in orange indicate higher overall expression while points in blue indicate lower overall expression.

Differential gene expression (DGE) analysis and gene set enrichment analysis (GSEA) using the Hallmark curated gene sets[7] revealed global and pathway-specific genomic differences between

poor responders and good responders to bevacizumab therapy, respectively. 9.5% of all protein coding genes were significantly differentially expressed between the two response groups (Figure 1A). The most differentially expressed genes included *MXRA5*, *FIGNL2*, *DPP10*, *SHD*, *IGLON5*, *SYT13*, *NCAN*, *SIX6*, *SCN3B*, *VGF*, *MMD2*, *B3GAT1*, *NAT16*, *USP43*, *ABCC8*, *ATCAY*, EXTL1, *KCNA6*, *TLX1*, *SCG3*, with the majority of differentially expressed genes being positively enriched in poor responders to bevacizumab therapy (Supplemental Table 2). Specific pathways similarly showed perturbations, with 23 gene sets showing significantly altered expression in poor responders to bevacizumab therapy (Figure 1B). Notably, only genes downregulated under KRAS pathway activation showed positive enrichment in poor responders to bevacizumab while some of the most downregulated gene sets included interferon gamma response, the mTORC1 genes, Myc targets, and interferon alpha response genes (Supplemental Table 3). Several of these pathways and gene sets have been previously shown to be involved in angiogenesis. Notably the mTOR pathway has been shown to activate under RAS mutation and is connected to angiogenesis via VEGF[8]. This provides further evidence for bevacizumab driven cellular adaptation. Specifically, the similar high degree of synteny between the KRAS and angiogenic pathways[9,10] suggested differential expression of angiogenic pathway genes may be a method of cellular bevacizumab evasion. To better understand the role of differential expression of angiogenic factors on bevacizumab therapy, the raw expression data of genes annotated under the Gene Ontology Angiogenesis[11] pathway was quantified (Figure 1C). Poor responders to bevacizumab therapy showed differential expression of several angiogenic factors, including *APOD*, *GATA4*, *KDR*, *ACVRL1*, *RAMP3*, *LAMA1*, *ADGRB1*, *JCAD*, *SFRP1*, *TAL1*, *PPP1R16B*, *NGFR*, *EPHB1*, *AMOT*, *CHRNA7*, *NPR1*, *EGR3*, *HOXB13*, *CAV1* (Table 1).

Angiogenesis Differential Gene Expression

Gene	*Fold.Change*	*P-value*	*Adjusted P-value*	*Mean Expression*
APOD	227.46	0.00	0.00	9745.38
GATA4	160.41	0.00	0.00	682.76
KDR	0.01	0.00	0.00	3358.70
ACVRL1	103.49	0.00	0.00	184.83
RAMP3	84.64	0.00	0.00	40.72
LAMA1	72.39	0.00	0.00	1030.16
ADGRB1	53.71	0.00	0.00	19203.15
JCAD	52.25	0.00	0.00	723.10

SFRP1	46.57	0.00	0.00	1223.68
TAL1	41.14	0.00	0.00	184.06
PPP1R16B	36.06	0.00	0.00	1187.25
NGFR	36.04	0.00	0.00	23550.01
EPHB1	31.78	0.00	0.00	3240.27
AMOT	30.63	0.00	0.00	2750.02
CHRNA7	21.96	0.00	0.00	64.28
NPR1	18.30	0.00	0.00	1308.78
EGR3	18.02	0.00	0.00	2077.38
HOXB13	17.86	0.00	0.00	2183.89
CAV1	0.06	0.00	0.00	6744.06

Table 1 List of differentially expressed angiogenic genes. Fold change represents the ratio of expression in poor responders to good responders to bevacizumab treatment.

3.2 EGR1 may drive poor response to bevacizumab in part through regulation of CHRNA7.

Figure 2 A. violin plot CHRNA7 proteomic data B. violin plot EGR1 proteomic data C. violin plot ACVRL1 proteomic data D. Picture of actual slide for CHRNA7 E. Picture of actual slide for EGR1.

Previous literature revolving around these angiogenic genes highlighted *CHRNA7* and *EGR1* as potential key players in the poor response to bevacizumab therapy. Specifically, *CHRNA7* has been shown to promote angiogenesis or tumor cell proliferation and migration through an *EGR1* dependent mechanism[12,13]. Additionally, prior research has demonstrated a mitigation of tumor cell migration following antagonization of the *CHRNA7* protein product α7 Nicotinic Acetylcholine Receptor subunit[14]. Moreover, the impact of altered expression of *CHRNA7* on bevacizumab response has been previously qualified outside of glioblastoma, with studies finding an increase in choroidal neovascularization paralleling an increased expression of *CHRNA7* under bevacizumab therapy *in vivo*[15]. Interestingly, α7-nAChR antagonist experiments found that α7-nAChR drives angiogenesis through an early growth response 1 (*EGR1*) dependent pathway[12]. Data in small cell lung cancer suggests that *EGR1* serves as a transcription factor for *CHRNA7* expression, positively driving its transcription and has similarly been shown to either directly or

indirectly regulate several of the other differentially expressed angiogenic genes under poor bevacizumab response, including *AMOT*[16], *RAMP3*[17], and *ACVRL1*[18].

Protein-level differences in expression of *CHRNA7* and *EGR1* were measured through immunohistochemistry to validate transcriptome level changes. *CHRNA7* and *EGR1* again showed upregulation in poor responders to bevacizumab by factors of x (Figure 2A) and y (Figure 2B), respectively. Another pro-angiogenic downstream target of *EGR1*, *ACVRL1*, was tested to assess the role of *EGR1* in broadly driving angiogenesis. *ACVRL1* showed a similar upregulation by a factor of z (Figure 2C). These data parallel the RNA-sequencing level results showing 22-fold upregulation of *CHRNA7*, 13-fold upregulation of *EGR1*, and 103-fold upregulation of *ACVRL1* in poor bevacizumab responders relative to good responders.

3.3 Differential expression of both CHRNA7 correlates with poor prognosis.

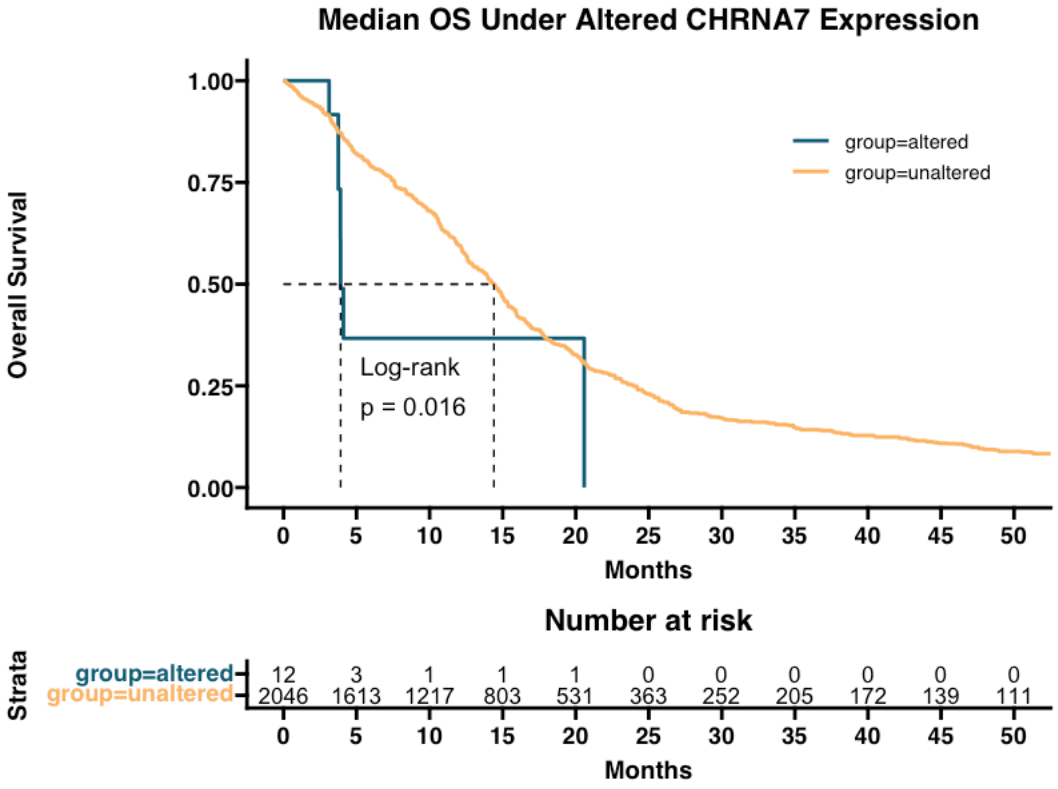

Figure 3 Kaplan Meier curve of glioblastoma patients with or without altered mRNA levels of *CHRNA7*. Log-rank survival analysis shows a significant difference in median overall survival.

Following validation of differential transcription and translation of *CHRNA7*, its pertinence to survival in glioblastoma was measured through analysis of clinical datasets curated through cBioPortal[19,20,21]. Patients with alterations in *CHRNA7* in glioblastoma showed significantly worse prognosis, with such patients having a median overall survival of around just 4 months (Figure 3).

In aggregate, our data suggests that response to bevacizumab delineates a distinct molecular phenotype of glioblastoma and highlights potential for patients' tumor-specific genomic characteristics for precision medicine.

4 Discussion

4.1 Clinical Significance

Currently, there is limited literature regarding genetic biomarkers predicting response to bevacizumab for treatment of recurrent glioblastoma. Existing biomarkers are relegated to MRI-dependent scans within the tumor microenvironment[22]. As aforementioned, identification of specific genes as biomarkers for poor responders to bevacizumab therapy can help determine potentially responsive or unresponsive patients, allowing them to transition to alternative therapies. Given the poor prognosis of glioblastoma, early identification of these patient populations can significantly improve median overall survival. Moreover, despite bevacizumab's inability to improve median overall survival in most patients, its ability to reduce brain edema through vascular normalization makes it a popular choice. Thus, retaining bevacizumab's anti-symptomatic effects while recovering its tumor-specific potency remains a tantalizing prospect. Beyond *CHRNA7*, genes involved in the differentially expressed pathways (including angiogenesis), have potential as therapeutic targets in combination with bevacizumab and can be the topic of future research.

4.2 Future Directions

While computational identification of differentially expressed genes can be used to delineate patients with predicted poor response to bevacizumab, it alone does not improve patient prognosis. In the long term, understanding the molecular mechanisms driving a good and a poor response to bevacizumab could highlight candidate targets for combination therapy, opening a new subset of patients to bevacizumab therapy through synthetic lethality. Thus, finding candidate molecular targets that when targeted would be additive or synergistic in effect with bevacizumab therapy, could improve median overall survival while retaining the anti-symptomatic benefits (enhanced quality of life) for patients with recurrent glioblastoma that are treated with bevacizumab. Better understanding the role of *CHRNA7* in glioblastoma tumor cell proliferation and migration through an *in vitro CHRNA7* knockout model generated via CRISPR-Cas9 will be crucial to understanding the underlying mechanism driving bevacizumab response. Based on successful validation studies (i.e., inhibition of proliferation and/or migration with knockdown of *CHRNA7*), the impact of *CHRNA7* knockout on bevacizumab response can be quantified *in vivo*. While *CHRNA7* shows promise as a potential target to recover response to bevacizumab, its transcription factor, *EGR1*, may play a more central role in regulating response. Thus, repeating the aforementioned experiments to validate *EGR1*'s role through a CRISPR interference[23] experiment can similarly lead to development of downstream therapeutic molecules.

4.3 Limitations

While our analysis did identify significant transcriptomic and proteomic level changes including potential contributors to bevacizumab response, limited sample size and variability amongst xenografts may confound our results. Moreover, due to current insurance practices, it is difficult to obtain recurrent glioblastoma tumors with differential response to bevacizumab, forcing artificial replication of bevacizumab response through changes in median overall survival. Additionally, biological differences between recurrent and primary tumors have been previously reported in glioblastoma[24], further confounding our analysis.

5 Appendix

5.1 Supplemental Figures

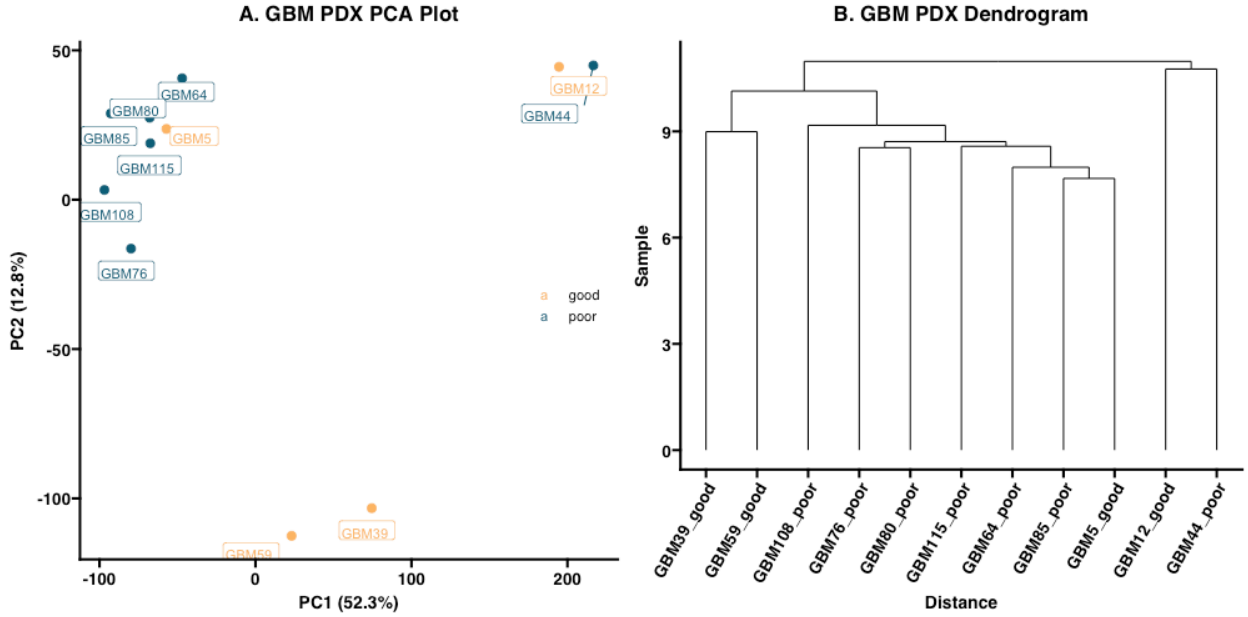

Supplemental Figure 1 A. The first two principal components of each mouse are plotted with color indicating the response group. Samples GBM44_poor and GBM5_good do not cluster in their respective group. B. The same data is shown as a dendrogram.

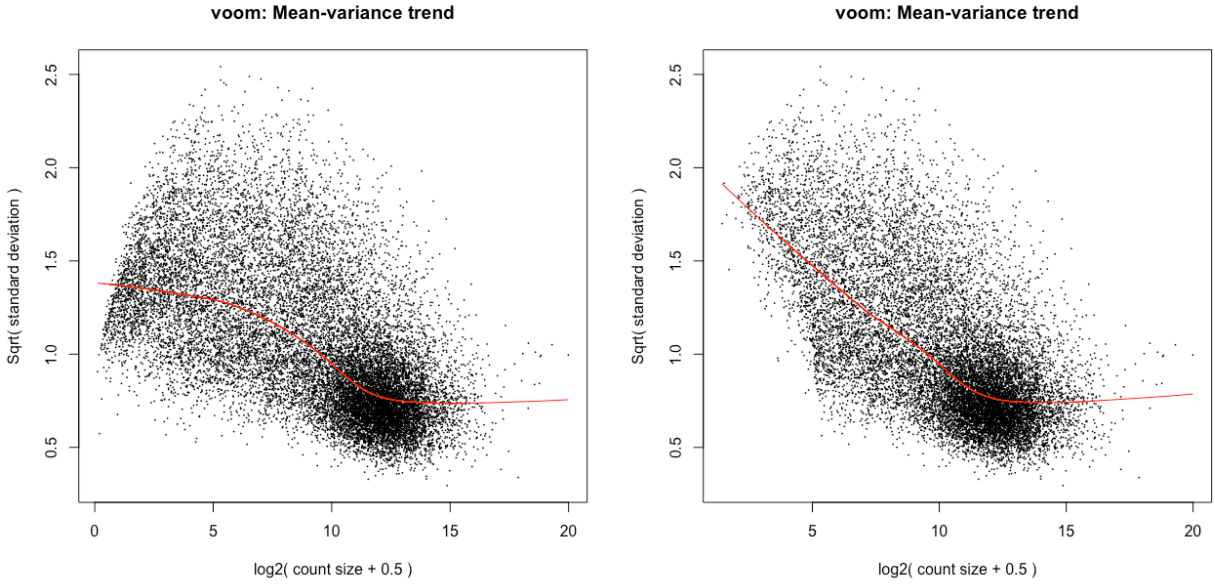

Supplemental Figure 2 Mean-variance trends before (left) and after (right) transcript filtering based on hyperparameter optimization.

5.2 Supplemental Tables

Supplemental Table 1 Glioblastoma patient derived xenograft samples reference table.

Study Design

Sample	*Group*	*SRA*
GBM64_poor	poor	SRR9294073.1
GBM76_poor	poor	SRR9294072.1
GBM80_poor	poor	SRR9294077.1
GBM85_poor	poor	SRR9294060.1
GBM108_poor	poor	SRR9294041.1
GBM115_poor	poor	SRR9294043.1
GBM12_good	good	SRR9294075.1
GBM39_good	good	SRR9294069.1
GBM59_good	good	SRR9294032.1

Supplemental Table 2 List of the top 20 differentially expressed genes identified through differential gene expression analysis. Fold change represents the ratio of expression in poor responders to good responders to bevacizumab treatment.

Differential Gene Expression

Gene	*Fold Change*	*P-value*	*Adjusted P-value*	*Mean Expression*
MXRA5	1868.27	0.00	0.00	1759.89
FIGNL2	1569.38	0.00	0.00	436.46
DPP10	1492.07	0.00	0.00	2903.70
SHD	1490.51	0.00	0.00	3325.96
IGLON5	1353.83	0.00	0.00	2933.21
SYT13	1308.00	0.00	0.00	925.22
NCAN	1187.78	0.00	0.00	38401.23
SIX6	1050.67	0.00	0.00	646.75

SCN3B	923.04	0.00	0.00	1313.92
VGF	878.53	0.00	0.00	27375.38
MMD2	784.09	0.00	0.00	300.90
B3GAT1	733.52	0.00	0.00	9828.08
NAT16	699.09	0.00	0.00	1335.63
USP43	683.91	0.00	0.00	816.73
ABCC8	630.66	0.00	0.00	2770.25
ATCAY	624.96	0.00	0.00	10365.40
EXTL1	621.35	0.00	0.00	622.66
KCNA6	619.83	0.00	0.00	1845.29
TLX1	570.41	0.00	0.00	795.25
SCG3	567.91	0.00	0.00	10645.30

Supplemental Table 3 List of the top 10 differentially expressed gene sets identified through gene set enrichment analysis. Positive normalized enrichment indicates upregulation in poor responders to bevacizumab. Genes listed in core enrichment are sorted in decreasing order of differential expression.

Gene Set Enrichment

Genset	*Normalized Enrichment*	*Adjusted P-value*	*Core Enrichment*
HALLMARK INTERFERON GAMMA RESPONSE	-2.34	0.00	IRF9/CMPK2/BPGM/CXCL11/IFIH1/PNPT1/USP18/JAK2/HLA-A/CASP3/IL7/MX2/MYD88/STAT1/NLRC5/CASP4/IFI44L/SPPL2A/PARP14/ST8SIA4/RTP4/MT2A/NOD1/IFI35/CASP8/EPSTI1/PTPN2/HERC6/PML/HIF1A/CASP7/IFIT2/PLSCR1/IRF1/PARP12/PTPN1/LGALS3BP/IFI44/RSAD2/UPP1/LAP3/SP110/NCOA3/ICAM1/EIF2AK2/IFITM2/DDX58/ZNFX1/RIPK1/PSMB10/IFITM3/IL15/OAS2/PSME

			1/PSMA2/MX1/NMI/IFIT3/VAMP5/FAS/NAMPT/PSMA3/IFI30/OASL/SOD2/PNP/ISG20/PSMB2/B2M/NFKB1/IFIT1/ISG15/NFKBIA/GBP4/MVP/IFI27/PSME2/TNFAIP2
HALLMARK MTORC1 SIGNALING	-2.45	0.00	RDH11/CCT6A/NIBAN1/STIP1/PITPNB/COPS5/LGMN/EEF1E1/EDEM1/HMBS/CACYBP/SLC9A3R1/BHLHE40/CYP51A1/USO1/RAB1A/DDX39A/CYB5B/PDK1/MTHFD2L/PLK1/BTG2/HSPA5/PSMA4/HSP90B1/SDF2L1/RPN1/SQLE/M6PR/GPI/FKBP2/G6PD/AK4/BUB1/GLRX/PSMD13/ERO1A/STC1/PSMG1/MAP2K3/ARPC5L/TBK1/EGLN3/POLR3G/ATP6V1D/SEC11A/GMPS/PRDX1/SSR1/PPIA/HSPA4/ENO1/HSPD1/GBE1/P4HA1/ELOVL5/ACTR3/PNO1/CALR/IMMT/GAPDH/LDLR/UBE2D3/PSMC2/GTF2H1/HSPE1/ETF1/STARD4/CD9/PSMB5/EIF2S2/EBP/PSMD12/PSMC4/NAMPT/PSMA3/IFI30/TPI1/CCNG1/ACTR2/PSMC6/GLA/PNP/SQSTM1/HPRT1/AURKA/RIT1/LDHA/ELOVL6/ALDOA/SLC2A1/PSMD14/PGK1
HALLMARK MYC TARGETS V1	-2.54	0.00	ORC2/EIF3B/DEK/DDX21/CNBP/TXNL4A/SRPK1/NME1/NOP56/CANX/RPL22/PRDX3/RPL14/SYNCRIP/COPS5/RPS10/EIF3D/VBP1/APEX1/HNRNPA2B1/TYMS/EIF1AX/RPS5/PTGES3/PCBP1/G3BP1/RPS2/EEF1B2/ILF2/POLE3/KARS1/PRPF31/TCP1/KPNA2/PWP1/YWHAE/EIF2S1/SSBP1/GOT2/PSMA4/RPLP0/SRSF1/TARDBP/EIF3J/UBA2/TRA2B/CUL1/AIMP2/SERBP1/RPL34/PCNA/NPM1/YWHAQ/RPS6/ERH/HNRNPC/DHX15/RACK1/VDAC1/SNRPD3/MRPL9/SSB/HSP90AB1/HDDC2/ACP1/UBE2L3/SNRPB2/PPM1G/PPIA/CDC20/EIF4E/LSM7/SLC25A3/HSPD1/PRPS2/RPL18/SRSF3/NOP16/CCT4/NDUFAB1/CCNA2/CCT7/PSMA2/HSPE1/SNRPD1/PSMD7/PSMD1/ETF1/PSMA1/GLO1/VDAC3/ABCE1/AP3S1/XRCC6/SRSF7/EIF4G2/EIF2S2/MAD2L1/H2AZ1/PSMC4/PSMD8/SNRPG/PSMC6/SNRPD2/PSMB3/PSM

			B2/HPRT1/LDHA/SNRPA1/PSMA6/PRDX4/PSMA7/PSMD14/PGK1
HALLMARK OXIDATIVE PHOSPHORYLATION	-2.47	0.00	NDUFA2/MRPS22/COX11/NDUFC2/PDHX/ATP6V0B/PRDX3/MRPL35/DLD/ATP5MC3/ACAT1/SDHC/BAX/NDUFB2/SUCLG1/ISCA1/COX7C/DLST/NDUFS4/NDUFS6/NDUFB5/MRPL11/NDUFB8/ATP6V1F/NDUFB3/ATP5MG/NDUFS1/GOT2/COX5B/ATP6V1E1/TIMM50/GPI/NDUFA8/MRPS12/MDH2/ATP5F1C/NDUFS8/VDAC2/DLAT/MRPS30/CASP7/ECHS1/TIMM8B/MGST3/ATP5ME/ATP5MF/UQCRC2/VDAC1/NDUFA9/ATP6AP1/HADHA/NDUFA3/AFG3L2/NDUFA7/UQCR10/CYCS/CPT1A/ATP6V1D/TIMM9/NDUFB4/ATP5PB/ATP5F1A/NDUFA4/NDUFB7/NDUFA6/UQCRFS1/SLC25A3/COX7A2/NDUFC1/TOMM22/ETFDH/COX4I1/HSD17B10/IMMT/SLC25A5/NDUFB1/OXA1L/NDUFAB1/TIMM17A/CYB5A/UQCRQ/GPX4/ETFA/ABCB7/PDP1/MDH1/ATP5PD/DECR1/COX6C/NDUFV2/PDHA1/UQCRH/GRPEL1/ATP6V0E1/UQCR11/AIFM1/FH/VDAC3/MRPL15/NQO2/COX6B1/NDUFA1/IDH3G/ECH1/ACAA2/HCCS/MPC1/NDUFB6/COX7B/COX7A2L/MRPL34/SDHB/ATP5F1E/LDHA/MRPS15
HALLMARK INTERFERON ALPHA RESPONSE	-2.23	0.00	WARS1/SAMD9L/TRIM25/IRF2/CD47/CXCL10/TRIM21/IRF9/CMPK2/CXCL11/IFIH1/PNPT1/USP18/SAMD9/IL7/PARP9/IFI44L/PARP14/CSF1/RTP4/IFI35/CASP8/EPSTI1/ELF1/HERC6/IFIT2/PLSCR1/IRF1/PARP12/LGALS3BP/IFI44/RSAD2/LAP3/SP110/EIF2AK2/IFITM2/GMPR/IFITM3/IL15/PSME1/MX1/NMI/IFIT3/PROCR/PSMA3/IFI30/OASL/ISG20/B2M/ISG15/IFITM1/GBP2/GBP4/IFI27/PSME2
HALLMARK PROTEIN SECRETION	-2.18	0.00	ANP32E/OCRL/GALC/TSG101/AP3B1/ARFGAP3/IGF2R/ARCN1/SCAMP3/BET1/PAM/USO1/GOLGA4/SEC31A/CLTC/RER1/M6PR/BNIP3/TMED10/ZW10/SOD1/COPB1/VPS4B/NAPA/SEC22B/YIPF6/RAB22A/ARF1/TMED2/LMAN1/SEC24D/

			ADAM10/CD63/ARFGEF2/TMX1/COPE/SNX2/ARFIP1/CLTA/AP2S1/RAB9A/AP3S1/ERGIC3/KRT18/GLA/LAMP2
HALLMARK FATTY ACID METABOLISM	-2.01	0.00	IDI1/SERINC1/RETSAT/NBN/SMS/DLD/RDH11/SDHC/SUCLG1/NTHL1/HSP90AA1/APEX1/DLST/ERP29/MIF/HMGCL/HSD17B11/HSD17B7/MDH2/GRHPR/G0S2/ACSL1/ACOT8/ECHS1/HADH/ACAT2/CRYZ/PTS/YWHAH/METAP1/CPT1A/EPHX1/ETFDH/ELOVL5/HSD17B10/ADSL/UROD/MDH1/PSME1/DECR1/RAP1GDS1/PDHA1/FH/IDH3G/ECH1/ACAA2/HCCS/H2AZ1/NSDHL/PRDX6/OSTC/LGALS1/S100A10/ACSL4/LDHA/ALDOA/ECI2
HALLMARK PI3K AKT MTOR SIGNALING	-2.00	0.00	PDK1/CLTC/HSP90B1/NOD1/ATF1/RALB/PPP1CA/MAP2K3/TBK1/MKNK1/EIF4E/ARF1/ARPC3/RIPK1/ACTR3/CALR/UBE2D3/YWHAB/ACTR2/SQSTM1/PPP2R1B/RIT1/SLC2A1/PFN1
HALLMARK KRAS SIGNALING DN	1.81	0.00	SOX10/CLSTN3/CAMK1D/TLX1/THRB/MACROH2A2/SLC29A3/GDNF/YBX2/MYH7/RYR1/KCNN1/GPR19/ARHGDIG/RGS11/COL2A1/THNSL2/ACTC1/YPEL1/RIBC2/ALOX12B/HSD11B2/TEX15/KCND1/FGFR3/MYO15A/PDE6B/SLC30A3/GAMT/SPTBN2/C5/NR4A2/DLK2/NRIP2/PDK2/ARPP21/SKIL/STAG3/TGM1/SYNPO/CPA2/WNT16/IDUA/MAST3/TFAP2B/SNCB/CHST2/DCC/EFHD1/PRODH/CPEB3

5.3 Reproducible scripts

https://github.com/roshanlodha/bevacizumab-response

5.4 References

1. Gil-Gil MJ, Mesia C, Rey M, Bruna J. Bevacizumab for the Treatment of Glioblastoma. Clin Med Insights Oncol 2013;7:123–35.

2. Weller M, Cloughesy T, Perry JR, Wick W. Standards of care for treatment of recurrent glioblastoma--are we there yet? Neuro-Oncol 2013;15(1):4–27.

3. Chamberlain MC. Bevacizumab for the Treatment of Recurrent Glioblastoma. Clin Med Insights Oncol 2011;5:117–29.

4. Cohen MH, Shen YL, Keegan P, Pazdur R. FDA drug approval summary: bevacizumab (Avastin) as treatment of recurrent glioblastoma multiforme. The Oncologist 2009;14(11):1131–8.

5. Müller-Greven G, Carlin CR, Burgett ME, et al. Macropinocytosis of Bevacizumab by Glioblastoma Cells in the Perivascular Niche Affects their Survival. Clin Cancer Res 2017;23(22):7059–71.

6. Kazazi-Hyseni F, Beijnen JH, Schellens JHM. Bevacizumab. The Oncologist 2010;15(8):819–25.

7. Liberzon A, Birger C, Thorvaldsdóttir H, Ghandi M, Mesirov JP, Tamayo P. The Molecular Signatures Database Hallmark Gene Set Collection. Cell Syst 2015;1(6):417–25.

8. Karar J, Maity A. PI3K/AKT/mTOR Pathway in Angiogenesis. Front Mol Neurosci 2011;4:51.

9. Matsuo Y, Campbell PM, Brekken RA, et al. K-Ras Promotes Angiogenesis Mediated by Immortalized Human Pancreatic Epithelial Cells through Mitogen-Activated Protein Kinase Signaling Pathways. Mol Cancer Res MCR 2009;7(6):799–808.

10. Hamarsheh S, Groß O, Brummer T, Zeiser R. Immune modulatory effects of oncogenic KRAS in cancer. Nat Commun 2020;11(1):5439.

11. angiogenesis Gene Ontology Term (GO:0001525) [Internet]. [cited 2021 Sep 23];Available from: http://www.informatics.jax.org/vocab/gene_ontology/GO:0001525

12. Brown KC, Lau JK, Dom AM, et al. MG624, an α7-nAChR antagonist, inhibits angiogenesis via the Egr-1/FGF2 pathway. Angiogenesis 2012;15(1):99–114.

13. Chen S, Kang X, Liu G, Zhang B, Hu X, Feng Y. α7-Nicotinic Acetylcholine Receptor Promotes Cholangiocarcinoma Progression and Epithelial-Mesenchymal Transition Process. Dig Dis Sci 2019;64(10):2843–53.

14. Pepper C, Tu H, Morrill P, Garcia-Rates S, Fegan C, Greenfield S. Tumor cell migration is inhibited by a novel therapeutic strategy antagonizing the alpha-7 receptor. Oncotarget 2017;8(7):11414–24.

15. Davis SJ, Lyzogubov VV, Tytarenko RG, Safar AN, Bora NS, Bora PS. The effect of nicotine on anti-vascular endothelial growth factor therapy in a mouse model of neovascular age-related macular degeneration. Retina Phila Pa 2012;32(6):1171–80.

16. Scheicher R, Hoelbl-Kovacic A, Bellutti F, et al. CDK6 as a key regulator of hematopoietic and leukemic stem cell activation. Blood 2015;125(1):90–101.

17. Lee JY, Kim JH, Bang H, et al. EGR1 as a potential marker of prognosis in extranodal NK/T-cell lymphoma. Sci Rep 2021;11(1):10342.

18. Gonzalez CR, Vallcaneras SS, Calandra RS, Gonzalez Calvar SI. Involvement of KLF14 and egr-1 in the TGF-beta1 action on Leydig cell proliferation. Cytokine 2013;61(2):670–5.

19. Cancer Genome Atlas Research Network. Comprehensive genomic characterization defines human glioblastoma genes and core pathways. Nature 2008;455(7216):1061–8.

20. Brennan CW, Verhaak RGW, McKenna A, et al. The somatic genomic landscape of glioblastoma. Cell 2013;155(2):462–77.

21. Zhao J, Chen AX, Gartrell RD, et al. Immune and genomic correlates of response to anti-PD-1 immunotherapy in glioblastoma. Nat Med 2019;25(3):462–9.

22. Stadlbauer A, Roessler K, Zimmermann M, et al. Predicting Glioblastoma Response to Bevacizumab Through MRI Biomarkers of the Tumor Microenvironment. Mol Imaging Biol 2019;21(4):747–57.

23. Larson MH, Gilbert LA, Wang X, Lim WA, Weissman JS, Qi LS. CRISPR interference (CRISPRi) for sequence-specific control of gene expression. Nat Protoc 2013;8(11):2180–96.

24. Maher EA, Brennan C, Wen PY, et al. Marked Genomic Differences Characterize Primary and Secondary Glioblastoma Subtypes and Identify Two Distinct Molecular and Clinical Secondary Glioblastoma Entities. Cancer Res 2006;66(23):11502–13.